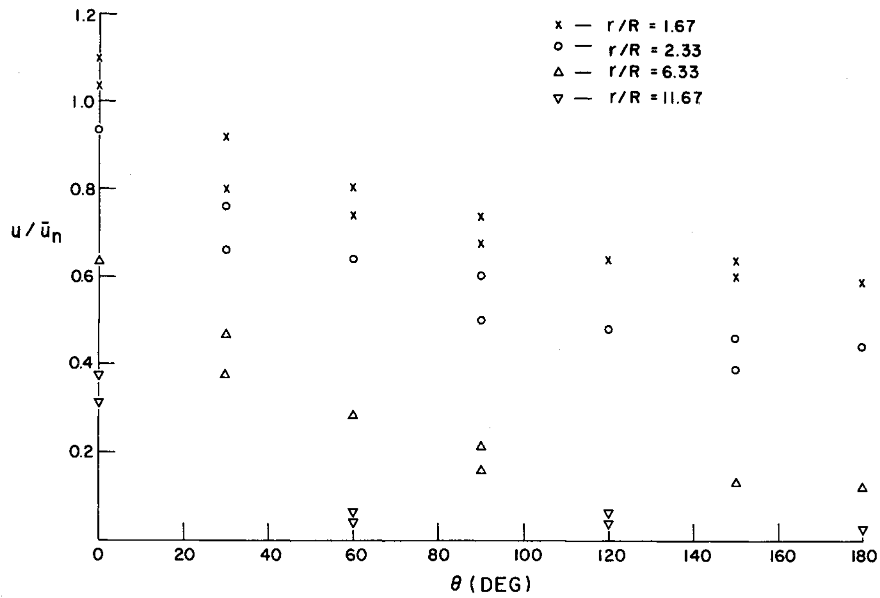

Fig. 4 Velocity distribution in the flowfield around an isolated eccentric porous tube.

The case of interest has a symmetric distribution of u_r which decreases monotonically from $\theta = 0$. With $-\pi \leq \theta \leq \pi$, $\omega < 0$ in $\theta < 0$ and $\omega > 0$ in $\theta > 0$. This distributed vorticity can be idealized as a series of vortex pairs, one above and one below the $\theta = 0$ axis, moving away from the tube surface. It is clear that as the flow expands from the surface, the vortices will tend to bend initially radial streamlines toward the thin wall section until they eventually reach an equilibrium displacement. In other words, the vortical flow from the tube surface must evolve into a jet with $\theta = 0$ as its axis.

III. Experiment

Due to practical difficulties in manufacturing the porous tubes with noncircular inner and outer contours, the porous tube for producing the ideal velocity distribution has not been developed. Instead, the eccentric porous tube studied in Ref. 2 was used in the present study. The tube used has dimensions of 0.95-cm o.d., 0.62-cm i.d., 0.11-cm thin wall thickness and 36-cm length. The porous tube has low porosity, designated by the manufacturer as having 0.5μ filtration, to attain a large pressure drop across the tube wall and thus insure uniform mass injection along the tube length. The predicted normal velocity distribution on the surface of the eccentric porous tube is shown in Fig. 2, together with the ideal velocity distribution that would lead to irrotational flow downstream of an array of 0.95-cm-o.d. tubes with 2.5-cm tube spacing. Here u_n is the normal velocity, $\bar{u}_n$ is the average velocity around the circumference of the tube, and θ is the angular location measured from the thin wall section.

Compressed nitrogen was fed in from both ends of the tube and the pressure inside the tube was maintained constant during each run. The entire tube was supported at 15 cm above the table. A constant temperature hot-wire anemometer (Thermo-Systems, Inc.) was used in conjunction with a linearizer for velocity measurement. 0.0008-cm (0.0003-in.) diam Wollaston wire was used on the hot wire probe and each probe was calibrated carefully to insure a linear net calibration curve.

Figure 3 shows the axial distribution of the velocity along $\theta = 0$ and at 0.32 cm from the tube surface. The pressure inside the porous tube was 8.27×10^6 dynes/cm^2 (120 psig). While there are variations in the velocity field, which can be attributed to small scale nonuniformities of the porous material coupled with jet coalescence effects, the axial average remains quite constant along the tube. Such axial average gives the average velocity at that particular location. Similar average velocities have also been obtained at different radial distances from the tube and angular locations from the thin wall section. The results are shown on Fig. 4, where r is the radial location measured from the center of the outer contour and R is the tube outside radius. For each r/R, the measured distribution shows that maximum velocity occurs at $\theta = 0$. The result also shows that the ratio $u_{\theta=0}/u_{\theta=180}$ increases as r/R increases. These two observations indicate that the flow around an isolated eccentric porous tube is a jet with its axis normal to the thin wall section of the porous tube.

In summary, a jet-like flowfield is theoretically predicted around an isolated porous tube with symmetric wall thickness distribution which is monotonically increasing from the thin wall section. Such behavior has been observed in the flow generated by an isolated eccentric porous tube. This particular behavior of a porous tube with non-uniform wall thickness distribution may provide a compact and convenient way of producing two-dimensional jet flow.

Acknowledgment

The authors wish to thank J. M. Avidor for his helpful suggestions. This work was supported by Naval Research under Contract No. N00014-76-C-0040.

References

[1] Avidor, J.M., Kemp, N.H., and Knight, C.J., "Experimental and Theoretical Investigation of Flow Generated by an Array of Porous Tubes," *AIAA Journal*, Vol. 14, Nov. 1976, pp. 1534-1540.

[2] Tong, K.-O., Knight, C.J., and Avidor, J.M., "Flow Generated by an Array of Eccentric Porous Tubes," *AIAA Journal*, Vol. 16, July 1978, pp. 747-749; also AIAA Paper 77-662, Albuquerque, N. Mex., June 1977.

Unsteady Flow Arising from Rotating Fluid above a Fixed Plane

W. H. H. Banks* and M. B. Zaturska*
University of Bristol, England

ONE special family of steady rotating flows which has been studied in some detail concerns the von Kármán disk problem and its generalizations: relative to a system of

Received April 24, 1979.

Index categories: Nonsteady Aerodynamics; Boundary Layers and Convective Heat Transfer—Laminar.

*Lecturer in Mathematics, School of Mathematics.

cylindrical polar coordinates (r, θ, z), fluid occupies the region $z>0$, while the plane $z=0$ is given a prescribed angular velocity ω about $r=0$ and the fluid has angular velocity Ω as $z \to \infty$. Assuming rotational symmetry, a similarity solution of the Navier-Stokes equations is possible provided that a certain system of ordinary differential equations, which involves the parameter $s=\Omega/\omega$, is satisfied. A great deal is known about the flow properties for various values of s.

The case $s=0$ corresponds to the rotating plane in fluid otherwise at rest, $s=1$ represents a solid-body rotation of fluid and plane, and $s=\infty$ ($\omega=0$) gives rise to the Bödewadt flow where the fluid rotates above the fixed plane $z=0$. Apart from a perturbation analysis about $s=1$, the solutions rely on the numerical integration of the system of equations. However, for $s=-1$, when the fluid and disk are counter-rotating, it has been shown by McLeod[1] that the steady similarity equations have no solution, and indeed, for a range of s near $s=-1$, no numerical solutions are known.

The situation has also been generalized to include unsteady effects: specifically it is assumed that for $t<0$ the plane and fluid are in solid-body rotation with angular velocity Ω and that at $t=0$ the plane is constrained to rotate with angular velocity ω about the same axis. The first complete numerical solution was given for the case $\Omega=0$ by Homsy and Hudson[2] and later by Katagiri.[3] Bodonyi and Stewartson[4] have reported an unsteady investigation for $s=-1$ and find evidence of a singularity occurring at a finite time. Also, Bodonyi[5] has recently reported some results for other values of s and, in particular, for $\omega=0$.

The present authors have considered a number of impulsive-start problems, including the case when $\omega=0$. Although there is certain qualitative agreement between Bodonyi's results and ours, there are some details that we would like to present.

The relevant equations for the velocity field are:

$$u_T + wu_z + u^2 - v^2 = -1 + u_{zz}$$

$$v_T + wv_z + 2uv = v_{zz} \tag{1}$$

$$2u + w_z = 0$$

where $r\Omega u$, $r\Omega v$, $(\nu\Omega)^{1/2} w$ are the radial, azimuthal, and axial velocity components, respectively, $(\nu/\Omega)^{1/2} z$ is the distance measured along the axis and T/Ω is the time. The initial and boundary conditions are:

$$T<0{:}\ u=w=0, v=1$$

$$T>0{:}\ u=w=v=0 \text{ on } z=0,$$

$$u \to 0, \quad v \to 1 \text{ as } z \to \infty \tag{2}$$

The procedure used for numerically integrating these equations is described in detail in Ref. 6; therefore, we will describe it only briefly here. Because of the singularity at $T=0$, we transform Eqs. (1) using the Blasius variable $z/2T^{1/2}$ to integrate to some time $T_0>0$ and then at T_0 revert to Eqs. (1) after transforming the coordinate z according to $\zeta=\log(1+z/2T_0^{1/2})$. The equations were replaced by their finite-difference equivalents using the Crank-Nicolson method. We note here that this procedure has been used by the present authors in previous work, including the problem of the unsteady flow occasioned by a rotating disk in counter-rotating fluid. The results of the latter investigations are such that, near the time of breakdown, they are consistent with the first term of the asymptotic solution given by Bodonyi and Stewartson. The ζ transformation has proven most useful in all these problems.

Our calculations were performed with a spatial step length $\Delta\zeta=0.1$ and a time step length $\Delta T=0.05$; the results were checked by repeating the calculations with $\Delta\zeta=0.05$. The

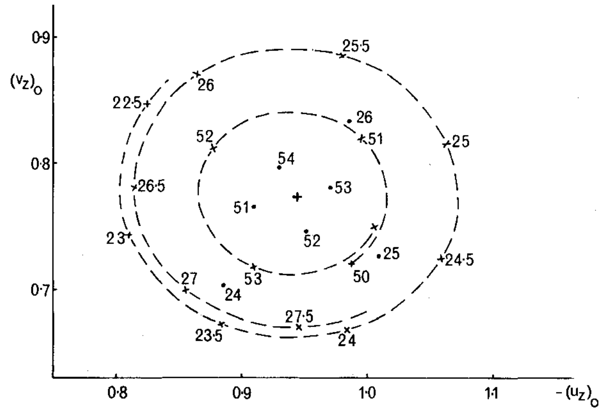

Fig. 1 Plot of $(v_z)_0$ vs $-(u_z)_0$ for various times indicated, •: Bodonyi's results' +: steady value (i.e., $T=\infty$).

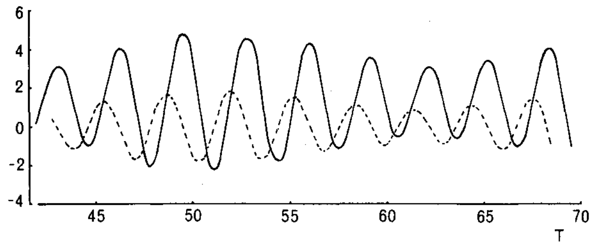

Fig. 2 Normal velocity at the boundary-layer edge, $w(\infty,T)$: ——; swirl displacement thickness, D: – – – –.

number N of spatial grid points used was adjusted as necessary at each time step to insure that at $N\Delta\zeta$ we satisfy $u_z \simeq 0$, $v_z \simeq 0$ in addition to $u=0$, $v=1$. We find that $N=N(T)$ and that for example, at $T=10$ it was sufficient to take $N=39$ ($z\simeq 48$), whereas at $T=82$ it was necessary to use $N=55$ ($z\simeq 244$) to achieve comparable accuracy. The extent of the penetration of the viscous effect is thus very large and as such exemplifies the usefulness of the logarithmic transformation. It may be opportune to note that the outer boundary condition was imposed at $z=60$ throughout the calculations of Bodonyi.

We discontinued the integration at $T=100$ because of the extremely slow convergence. The latter is demonstrated by plotting $(v_z)_0$ vs $-(u_z)_0$ in Fig. 1; we also give some of Bodonyi's results for comparison, and would suggest that the reason for his apparently faster convergence is probably because the outer boundary condition was imposed at $z=60$, thereby "cramping" the calculation. Our results for T near 100 are fairly close to those of Bodonyi with T near 50—they are not plotted in Fig. 1 to avoid confusion. The behavior of $(u_z)_0$ and $(v_z)_0$ as functions of T are of damped oscillatory form—the decay of the amplitude of the oscillation is monotonic. However, a property of the flowfield that is even more influenced by "cramping" the range of the calculation is $w(\infty,T)$, the normal velocity at the edge of the bondary layer. We find that $w(\infty,T)$ also oscillates with T, although the decay of the amplitude of the oscillation is non-monotonic; this was checked by repeating the calculation with $\Delta T=0.025$ over an interval of 14 time units. This property of $w(\infty,T)$ is illustrated in Fig. 2. Also shown is the swirl displacement thickness $D=\int_0^\infty (1-v)\mathrm{d}z$ which exhibits the same behavior. We note that, although the viscous penetration increases some 500%, the displacement thicknesses do not change by as much because of the oscillation of the velocities about their values at $z=\infty$.

It is found that with a spatial step length of 0.1, the steady values for $(u_z)_0$, $(v_z)_0$, and $w(\infty,T)$ are -0.939, 0.773, and 1.359, respectively; these are in reasonable agreement with the exact values -0.942, 0.773, and 1.349. We note that in the unsteady problem $(u_z)_0$ and $(v_z)_0$ oscillate about their steady values and appear to be exactly one-quarter period out of phase. This is also the case for $w(\infty,T)$ and D. A phase change in the skin-friction components occurred in a problem also considered by Homsy and Hudson: they analytically investigated the unsteady development of almost solid-body rotation, i.e., $s=1-\epsilon$, $|\epsilon|\ll 1$. It can be shown from their results that the departures of $(u_z)_0$ and $(v_z)_0$ from their steady values are $(4\sqrt{\pi}T^{3/2})^{-1}\epsilon\cos 2T$ and $(4\sqrt{\pi}T^{3/2})^{-1}\epsilon\sin 2T$, respectively, i.e., a phase difference of $\pi/4$.

It is hoped that the results of other investigations will be published in the near future.

References

[1] McLeod, J.B., "A Note on Rotationally Symmetric Flow Above an Infinite Rotating Disc," *Mathematika*, Vol. 17, 1970, pp. 243-249.

[2] Homsy, G.M. Hudson, J.L., "Transient Flow Near a Rotating Disk," *Applied Science Research*, Vol. 18, 1968, pp. 384-397.

[3] Katagiri, M., "Flow Due to Impulsive Rotation of Infinite Disk," *The Physics of Fluids*, Vol. 17, 1974, pp. 1463-1464.

[4] Bodonyi, R.J. and Stewartson, K., "The Unsteady Laminar Boundary Layer on a Rotating Disk in a Counter-Rotating Fluid," *Journal of Fluid Mechanics*, Vol. 79, 1977, pp. 669-688.

[5] Bodonyi, R.J., "On the Unsteady Similarity Equations for the Flow Above a Rotating Disc in a Rotating Fluid," *Quarterly Journal of Mechanics and Applied Mathematics*, Vol. 31, 1978, pp. 461-472.

[6] Banks, W.H.H. and Zaturska, M.B., "The Collision of Unsteady Laminar Boundary Layers," *Journal of Engineering Mathematics*, Vol. 13, 1979, pp. 193-212.

Large-Amplitude Fluctuations of Velocity and Incidence on an Oscillating Airfoil

Daniel Favier,* Jean Rebont,† and Christian Maresca‡
Institut de Mécanique des Fluides de Marseille, Marseille, France

Introduction

DUE to the complexity of unsteady effects, the three-dimensional aerodynamic behavior of a helicopter blade-section in forward flight has been extensively investigated in the course of the last few years.[1] Recent results[2] have shown that unsteady flows over the rotor blade can be modeled through two-dimensional oscillating airstreams over pitching airfoils. Therefore, most of the experimental and theoretical studies undertaken on this topic have tackled the problem by investigating unsteady flows for airfoils oscillating either in pitch,[3-5] or in translation parallel or normal to the undisturbed airstream.[6-8] A proper simulation of the flow surrounding the rotor blade requires considering incidence oscillations combined with simultaneous velocity fluctuations of the airstream. A recent work[9] has presented surface pressure measurements performed on a pitching airfoil in a fluctuating airstream. Unsteady effects are observed from the pressure distributions obtained at the same instantaneous angle of attack, with and without velocity oscillations of the airstream. In the present study, unsteady flow features due to large-amplitude fluctuations of both velocity and incidence induced by an airfoil executing cyclic time-dependent fore-and-aft translations, are investigated from lift, drag, and skin-friction measurements.

Received Dec. 26, 1978; revision received May 4, 1979.

Index categories: Nonsteady Aerodynamics; Jet, Wakes, and Viscid-Invicid Interactions.

*Research Scientist, National Center of Scientific Research.
†Research Engineer, National Center of Scientific Research.
‡Senior Research Scientist, National Center of Scientific Research.

Experimental Setup

The tests were conducted in a low-turbulence (<0.2%) open circuit wind tunnel (0.5×1×3 m). Under steady flow conditions, the range of static Reynolds numbers $Re_c=V_\infty c/\nu$ was $5.7\times10^4\leq Re_c\leq 4\times10^5$. The model consisted of a rectangular wing (span $l=0.495$ m and chord $c=0.3$ m), with a NACA 0012 profile with an angle of steady stall incidence of about 12 deg. This airfoil was supported by a frame oscillating sinusoidally in translation of amplitude A and rotational frequency $\omega=2\pi f$ which could be obtained in the ranges: $0\leq A\leq 0.17$ m and $0\leq f\leq 5$ Hz. Consequently, the reduced amplitude $\lambda=A\omega/V_\infty$, and the reduced frequency $k=c\omega/2V_\infty$ were respectively varied from 0 to 1.2 and from 0 to 1.6.

As exemplified on the diagram of Fig. 1, the static angle of attack α_0 is set up anywhere between −25 deg and 25 deg; and the airfoil is oscillating in translation along the X_δ oscillation axis. The angle δ between the X_δ axis and the freestream direction can be adjusted from 0 deg to 90 deg. When $\delta=0$ deg (or $\delta=90$ deg), the airfoil oscillates in translation parallel (or normal) to the undisturbed airstream. The angle i between the resultant velocity V and the chord airfoil is defined by:

$$i=\alpha_0-i_0 \text{ and } i_0=\text{arctg}[\lambda\cos\omega t\sin\delta/(1+\lambda\cos\omega t\cos\delta)] \quad (1)$$

The amplitude of fluctuating velocity is given as follows:

$$V^2=V_\infty^2(1+2\lambda\cos\omega t\cos\delta+\lambda^2\cos^2\omega t) \quad (2)$$

So, large-amplitude fluctuations of both velocity and incidence can be obtained with the maximum incidence coinciding with the minimum velocity. For two static angles of attack $\alpha_0=20$ deg and $\alpha_0=6$ deg, Fig. 1 gives the periodic variations of resultant velocity V and incidence i vs ωt, in the following conditions: $\delta=17$ deg; $\lambda=0.744$; $k=0.66$. As an example it can be seen that for $\alpha_0=20$ deg the instantaneous

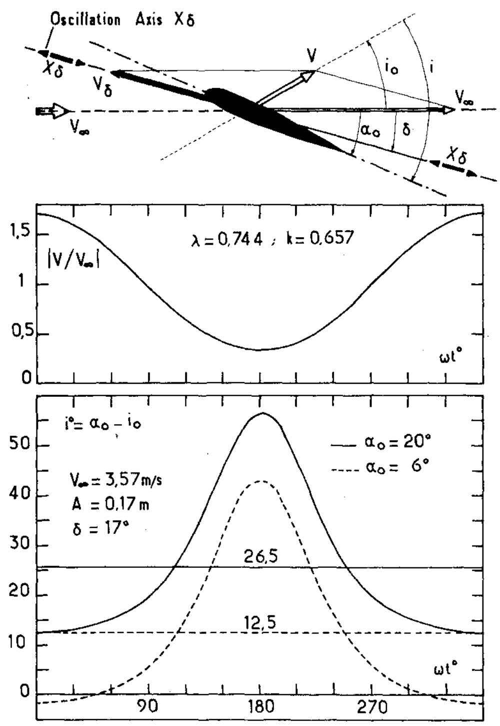

Fig. 1 Amplitude fluctuations of velocity and incidence.